Journal of Alloys and Compounds 727 (2017) 297–303

Contents lists available at ScienceDirect

Journal of Alloys and Compounds

journal homepage: http://www.elsevier.com/locate/jalcom

Enhanced tensile plasticity of Zr based bulk metallic glasses by a stress induced large scale flow

J. Dong [a, c, 1], M. Gao [b, 1], Y. Huan [a, c, *], Y.H. Feng [a], W. Liu [a], W.H. Wang [b]

[a] State Key Laboratory of Nonlinear Mechanics (LNM), Institute of Mechanics, Chinese Academy of Sciences, Beijing 100190, China
[b] Institute of Physics, Chinese Academy of Sciences, Beijing 100190, China
[c] School of Engineering Science, University of Chinese Academy of Sciences, Beijing 100049, China

ARTICLE INFO

Article history:
Received 7 June 2017
Received in revised form
31 July 2017
Accepted 6 August 2017
Available online 9 August 2017

Keywords:
Bulk metallic glasses
Large scale flow
Tensile plasticity
Laser-engraving
Finite element modeling

ABSTRACT

Tensile plasticity in a Zr-based bulk metallic glasses is achieved through a stress induced large-scale flow. The large-scale flow is activated in a complex stress field which is produced by introducing micro-pits array on specimen surfaces using a laser engraving technique. A flame-like fracture morphology with bigger size (about 10 μm in height) is observed on the fracture surface of specimen, indicating that the size of flow here is far beyond the size of that induced by shear bands. Theoretical analysis accompanied with finite elements modeling (FEM) reveal that the form of high shear zones agrees well with that of the large-scale flow, suggesting that the flow form is changed by the complex stress field. After a comprehensive analyze, the intense shear and suppressing shear bands are concluded to be the two necessary conditions for the stress induced large scale flow.

1. Introduction

Bulk metallic glasses (BMGs) have excellent physical, chemical, and mechanical properties, such as the large elastic limit, high strength and hardness. However, the wide spread application of BMGs as new structural engineering materials is severely stymied by the poor ductility and fatigue resistance [1–7]. Upon yielding, the flow in BMGs is highly localized into a narrow (10–20 nm in thickness) shear band at room temperature [8,9]. Under tensile load, the shear band will rapidly extend to a crack, causing catastrophically fracture. However, in the constrained stress field such as compression and bending, considerable plastic in BMGs can be achieved by multiple shear bands [10–14]. Based on this mechanism, substantial efforts have been made to enhance the tensile ductility of MGs, such as introducing heterostructures [15], notching [16,17], surface treatment [18,19] and cold working [20]. Nevertheless, the flow is still constrained in shear band and the ductility is also carried by multiple shear bands. Many studies also have reported that nano-scale MGs sustain uniform plastic flow such as the necking and stable shear flow deformation just like ductile crystalline metals under tensile loading [21–23]. However, it seems as if the flow in BMGs can only exist in nano-scale at room temperature.

By now, the homogeneous flow in BMGs is detected only when the temperature is elevated to the value above or at least close to the glass transition temperature. However, in the frame of the Landscape theory the flow process corresponds to the disappearance of local potential energy minima, which can be activated by thermal energy and stress [24,25]. Similar results also have been reported in the flow unit theory on atomic scale. The flow phenomenon in metallic glasses is thought to origin from the liquid-like units or flow units, which can be activated by temperature or stress [26–28]. These all indicate that the stress have the same effects as thermal energy in metallic glasses flow activation and the large-scale flow also can be obtained through stress activation at room temperature. However, the stress induced flow is still easy to appear in the form of shear bands even in the stress concentration zones [15–17].

In this study, a stress induced large scale flow in a $Zr_{65}Al_{10}Ni_{10}Cu_{15}$ BMG is achieved by a specially designed stress field at room temperature. The flow is activated in the form of many large flow events instead of a single shear band. Tensile plasticity is also achieved through large-scale flow rather than multiple shear

* Corresponding author. State Key Laboratory of Nonlinear Mechanics (LNM), Institute of Mechanics, Chinese Academy of Sciences, Beijing 100190, China.
E-mail address: huany@lnm.imech.ac.cn (Y. Huan).
[1] These authors contributed equally to this work.

http://dx.doi.org/10.1016/j.jallcom.2017.08.046
0925-8388/

bands. The underlying mechanism and the necessary conditions for the stress induced large scale flow are discussed.

2. Experimental methods

The pre-alloys for Zr-based BMG specimens with a nominal chemical composition of $Zr_{65}Al_{10}Ni_{10}Cu_{15}$ were prepared by arc melting appropriate amounts of constituting elements under a Ti-gettered argon atmosphere and casted into $1^t \times 10^w \times 50^l$ mm^3 plates by a copper mold suck-casting method. Then the plates were polished and cut into dog bone shaped specimens with a gauge section of $0.9^t \times 2.7^w \times 22^l$ mm^3. The polished dog bone specimen is treated by a laser-engraving (L-E) method. As shown in Fig. 1, bullet shaped micro pits with designed spatial distribution array were sculptured on both surfaces of specimen using a Picosecond laser TruMicro 5025. The fully amorphous structures of both as-cast and laser-engraved (L-E) specimens were ascertained by X-ray diffraction (XRD) and differential scanning calorimeter (DSC). XRD patterns show broad diffraction humps with no detectable crystalline Bragg peak, indicating that laser working did not induce any crystallization in specimens. Tensile tests were performed on an Instron ElectroPuls E10000 test instrument (equipped with a video extensometer) at a quasi static strain rate of about 1×10^{-4}s^{-1}. After test, the fracture morphology was examined using a scanning electron microscope (SEM).

3. Results and discussion

3.1. Stress-strain curves and fracture morphology

Tensile stress-strain curves for the Laser engraved (L-E) specimen and as a comparison, for the as-cast specimen are shown in Fig. 2. One can see that the as-cast specimen exhibits a tensile elastic strain of 2% and catastrophically fractured at a stress of 1600 MPa, which is a typical feature of monolithic BMGs [29].

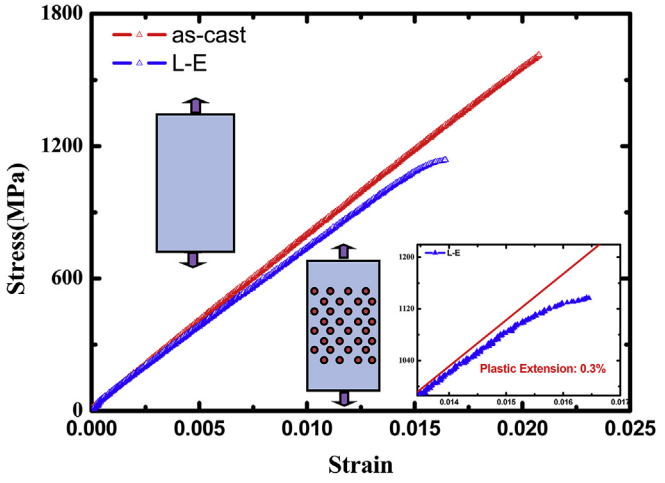

Fig. 2. The tensile stress-strain curves of as-cast and L-E specimens, respectively. Inset: the L-E specimen exhibits a plastic elongation of 0.3% at the moment of fracture.

However, the L-E specimen with designed micro architectures shows obvious plastic elongation at the moment of fracture as shown in the inset of Fig. 2. Meanwhile, no serration flow behaviors are observed in the plastic extension segment of the L-E specimen, which is different from that in compression, bending and some tensile tests [12–20]. It indicates that the plastic elongation here is not induced by the interaction of multiple shear bands. It should be mentioned that the reduce in the tensile stress level of the L-E specimen is essentially results of the reduction in effective cross section. Through a careful calculation, it can be found that the effective cross section of the L-E specimen is about 12.7% than that of the as-cast specimen. The true fracture stress of the L-E specimen is modified to 1520 MPa, which is also closed to the fracture stress of the as-cast specimen.

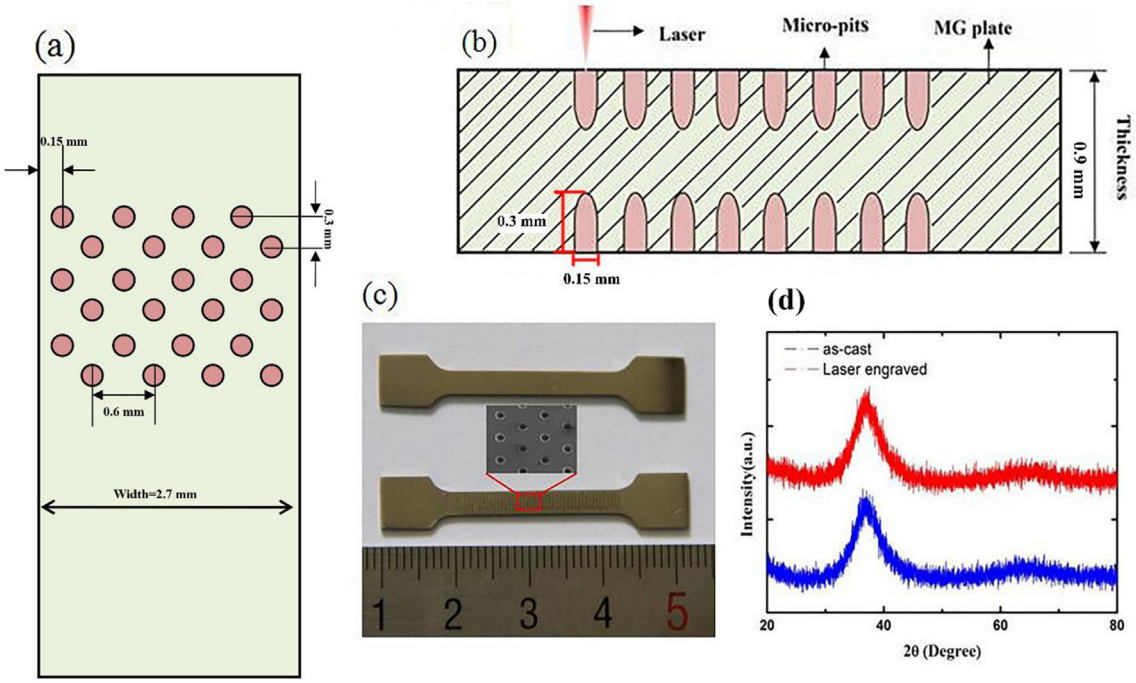

Fig. 1. (a) and (b) The Bullet shaped micro pits worked on both surfaces of plates using a laser-engraving technology. (c) The dog bone shaped as-cast and Laser engraved (L-E) specimens. (d) XRD patterns confirming the fully amorphous structure of the as-cast and (L-E) specimens.

SEM observations reveal significant difference in fracture morphology of the as-cast and L-E specimens after tensile test as shown in Fig. 3. It can be seen that the formation and propagation of a major shear band dominate the fracture process in the as-cast specimen. The tensile fracture angle between the loading axis and the fracture plane is about 52° (Fig. 3(a)), which is the typically fracture morphology caused by the major shear band for BMGs under tensile loading. In the L-E specimen, the fracture happened along a diagonal row of micro pits at an angle of 60° with respect to the loading axis (Fig. 3(b)), suggesting that the fracture process is mainly dominated by the micro pits rather than the major shear band. A radial shaped vein-like pattern, which is common on BMGs tensile fracture surfaces, is visible on the fracture surface of the as-cast specimen (Fig. 3(c) and (e)). Differently, plenty of flame-like cones are observed on the fracture surface of the L-E specimen (Fig. 3(d) and (f)). Compared with the radial shaped vein, it is obvious that these flame-like cones have a larger size (about 10 μm in height) as shown in Fig. 3(f).

The various patterns on BMGs fracture surfaces are the results of the material flow, which is caused by the high energy release at the moment of fracture [30,31]. The forms of these fracture morphology are closely related with the scale of material flow. The radial shaped vein of the as-cast specimen is a representative fingerprint induced by a major shear band in BMGs tensile fracture. By comparison, it can be concluded that the L-E specimen undergoes a larger scale viscous flow than that in the as-cast specimen. The scale of viscous flow in the L-E specimen is enough to be captured by the testing sensor, causing the obvious plastic extension in the tensile stress-strain curve. In addition, no multiple shear bands are observed on the fracture surface of the L-E specimen as shown in Fig. 3 (b), confirming that the tensile plastic for the L-E specimen is not the result of multiple shear bands.

3.2. Simulation and theory analysis

It is interestingly found that the flame-like cones mainly

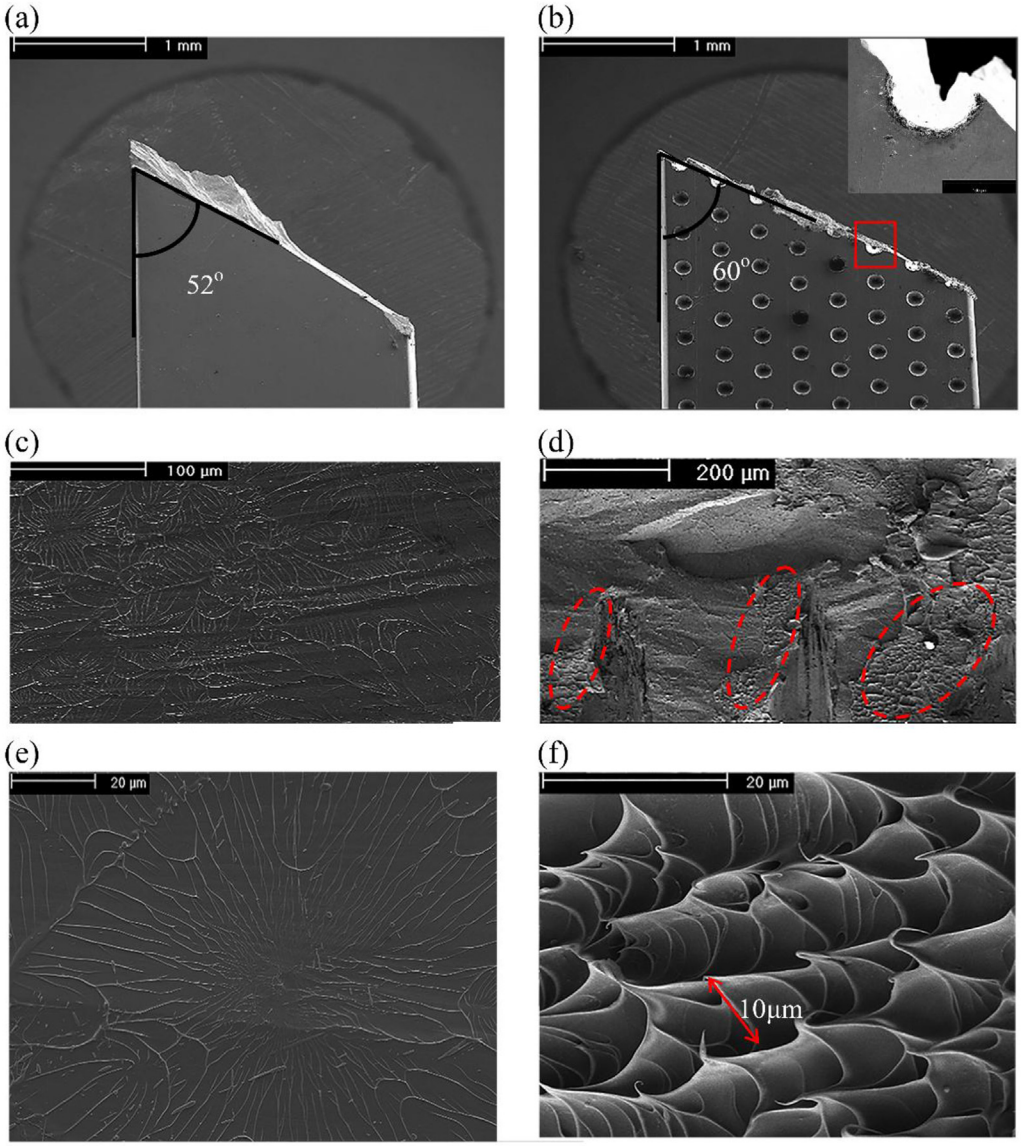

Fig. 3. (a) The as-cast specimen fractured along a major shear band at an angle of 52°. (b) The L-E specimen is influenced by the micro-pits and fractured along a diagonal row at an angle of 60°. (c) and (e) The radial shaped vein on the fracture surface of the as-cast specimen. (d) The flame-like cones distributing near the side and bottom of micro-pits on the fracture surface of the L-E specimen. (f) A close view to the flame-like cones on the L-E specimen.

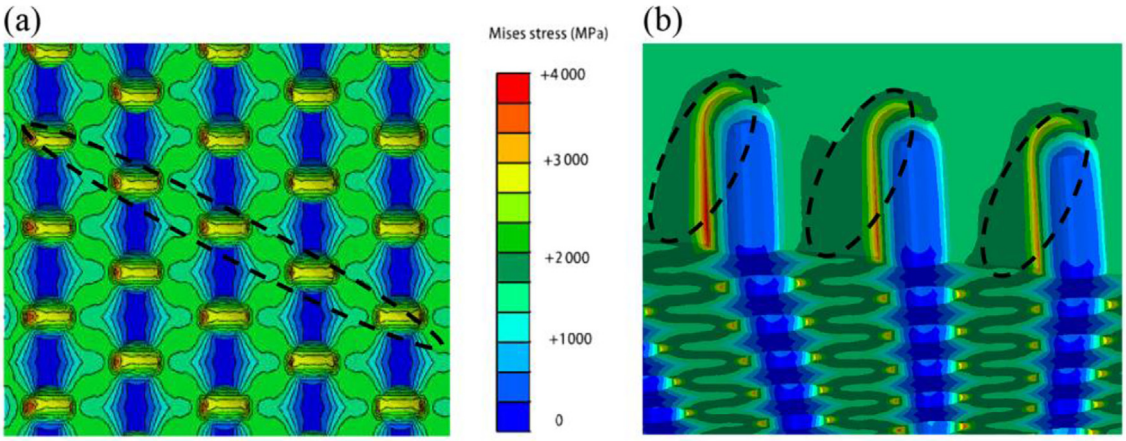

Fig. 4. The simulation results of the stress field in L-E specimen under tensile load. (a) The disorganized stress field caused by micro-pits array. (b) The high energy zones near the side and bottom of micro-pits on the fracture surface.

distribute at the bottom and the edge of the bullet shaped pits. The stress field for the L-E specimen under tensile load is studied using Finite element modeling (FEM). As shown in Fig. 4(a), simulation results clearly reveal that the stress field of the L-E specimen become disorganized due to the micro-pits array. One can see that many energy concentration zones are formed near the micro pits on the fracture surface as shown in Fig. 4(b). Compared with Fig. 3(d), it is found that the location of these energy concentration zones is agreed well that of the flame-like cones. It indicates that the flame-like cones in the L-E specimen is generated by the high stress around micro-pits. Indeed, the high stress is a necessary condition for activing material flow in BMGs. However, multiple shear bands are still not avoided even in stress concentration zones according to previous researches [15–17], which is different from the phenomenon here.

A further analysis for stress field of the L-E specimen is conducted. As shown in Fig. 5(a), we can see that the edge and the bottom of micro pits on the fracture surface acted as an in-plane shear (Mode II) crack and an out-of-plane shear (Mode III) crack at the moment of fracture, respectively.

Based on elastic theory, the analysis stress field around the crack tip in X-Y plane can be written as the forms shown in Eq. (1) and Eq. (2) for Mode II crack and Mode III crack, respectively.

$$\begin{cases} \sigma_x = -\dfrac{K_{II}}{\sqrt{2\pi r}}\sin\dfrac{\theta}{2}\left(2+\cos\dfrac{\theta}{2}\cos\dfrac{3\theta}{2}\right) \\ \sigma_y = \dfrac{K_{II}}{\sqrt{2\pi r}}\sin\dfrac{\theta}{2}\cos\dfrac{\theta}{2}\cos\dfrac{3\theta}{2} \\ \tau_{yx} = \dfrac{K_{II}}{\sqrt{2\pi r}}\cos\dfrac{\theta}{2}\left(1-\sin\dfrac{\theta}{2}\sin\dfrac{3\theta}{2}\right) \end{cases} \tag{1}$$

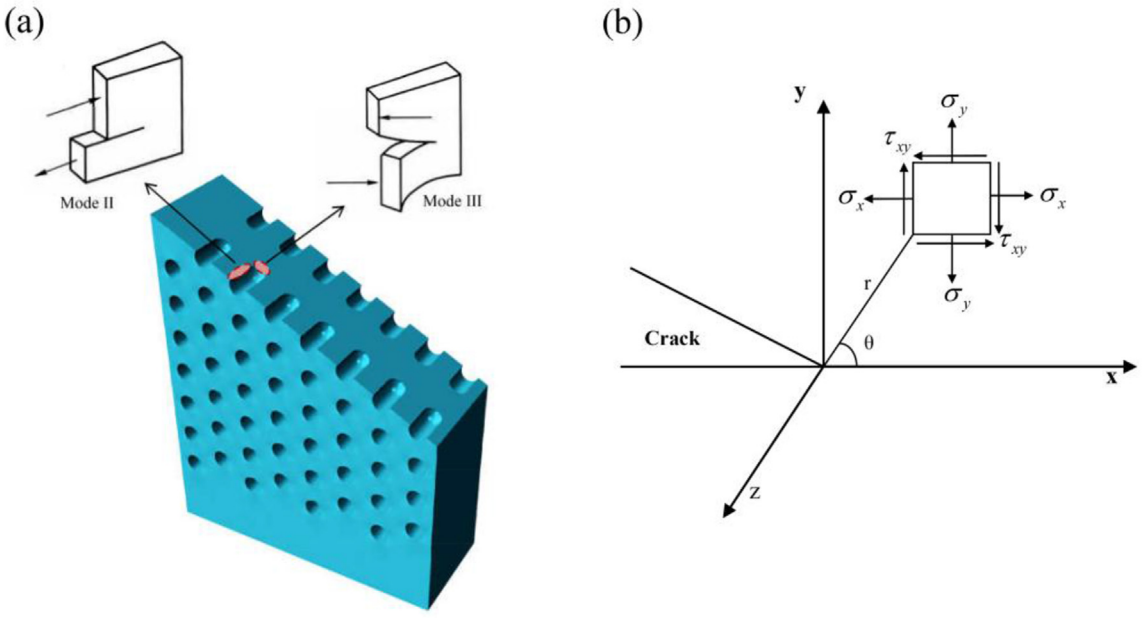

Fig. 5. (a) The edge and the bottom of micro-pit acting as an in-plane shear (Mode II) crack and an out-of-plane shear (Mode III) crack on the fracture surface at the moment of fracture sliding, respectively. (b) The stress element around the tip of crack which propagates along the X direction.

$$\begin{cases} \tau_{xy} = \dfrac{K_{III}}{\sqrt{2\pi r}}\cos\dfrac{\theta}{2} \\ \tau_{zx} = -\dfrac{K_{III}}{\sqrt{2\pi r}}\sin\dfrac{\theta}{2} \end{cases} \quad (2)$$

where K_{II} and K_{III} are stress intensity factors for Mode II crack and Mode III crack, respectively. The (r, θ) is a polar coordinate with the origin at crack tip as shown in Fig. 5(b). X is the crack propagation direction, Y is the normal crack direction and Z is the out-of-plane direction. Along the crack propagation direction x, where $\theta = 0$, the stress field became the forms shown in Eqs. (3) and (4) for Mode II crack and Mode III crack, respectively.

$$\begin{cases} \sigma_x = 0 \\ \sigma_y = 0 \\ \tau_{xy} = \dfrac{K_{II}}{\sqrt{2\pi r}} \end{cases} \quad (3)$$

$$\begin{cases} \tau_{xy} = \dfrac{K_{III}}{\sqrt{2\pi r}}. \\ \tau_{zx} = 0 \end{cases} \quad (4)$$

We can see that both the Mode II crack and the Mode III crack generate will generate a pure shear stress field on the fracture surface along the crack evolution direction. The high shear stress around the crack tip is the energy source of the large material flow in the L-E specimen.

The flow mechanism in BMGs during deformation is also closely related to the micro-structures, or more precisely, is related to the energy induced structure evolution. As we know, BMGs are prepared by fast quenching liquid through glass transition. In the fast quenching process large numbers of defects are frozen in, forming an inhomogeneous structure [32–34]. According to the flow unit theory, these frozen defects are nanosize inelastic liquid-like sites defined as flow units which exhibit a lower packing density, lower elastic modulus and higher energy dissipation rate [35–38]. The MGs structure can be regarded as inelastic soft units embedded in an elastic hard matrix, as is shown in Fig. 6.

These liquid-like flow units are considered as the basic carrier of flowing. With the local shear strain increasing, more flow units are activated and the size of existed flow units also become larger [28,34]. Finally, these units will combine with each other and form local flow. The whole process can be depicted as flow units activation, multiplication and percolation, as shown in Fig. 6.

The energy distribution is not absolutely uniform on the whole specimen during deformation. Local flow will firstly occur at high energy point which is thought to be the initial point of shear band. In the as-cast specimen, the stress field is uniform and the local flow is mainly resulted from the high energy point caused by structural heterogeneity or surface defect, as illustrated in Fig. 7(a). The deformation space is enough to dissipate energy in the unconstrained tensile stress field. Once local flow happens, it will rapidly extend into a major shear band (Fig. 7(a)) and then evolves into a crack, causing catastrophic fracture without formatting other shear bands.

In the L-E specimen the stress field becomes more complex because of the micro pits array as shown in Fig. 7(b). As mentioned above, shear concentration zones are generated around the edge and the bottom of the micro pits. In these regions, more and more flow units are activated by intense shear. Finally, these flow units percolated with each other and form local flow as shown in the left part of Fig. 7(b). From the right part of Fig. 7(b), one can see that flow in the L-E specimen occurs in the form of many large flow events rather than a major shear band. This is owned to the surrounding irregular stress field. As shown in Fig. 7(b), it is can be seen that the stress origination is changed in the stress field surrounded micro-pts, which prohibits the local flow from extending to a major shear band.

The differences of flow forms between the as-cast specimen and the L-E specimen is owed to the different form of high shear stress. In the uniform tensile stress field of the as-cast specimen, the theory angle of maximum shear stress plane is 45° with respect to the loading axis and shear band is also easy to occur around the maximum shear stress plane. However, in complex stress field of the L-E specimen, high shear stress mainly concentrate on the regions around the micro-pits and flow is also easy to occur in the form of large flow events. It should be realized that the flow in the as-cast and the L-E specimen have the same origin and are just different in forms because of the different shear stress field.

4. Conclusion

Tensile plasticity of BMGs is enhanced by a stress-induced large scale flow which is achieved by a special designed stress field. The intense shear and complex stress field are concluded to be the two necessary conditions for the large scale flow. The intense shear can active more flow units, forming the initial flow. Once the initial flow occurs, it will be prohibited extending into shear band by the

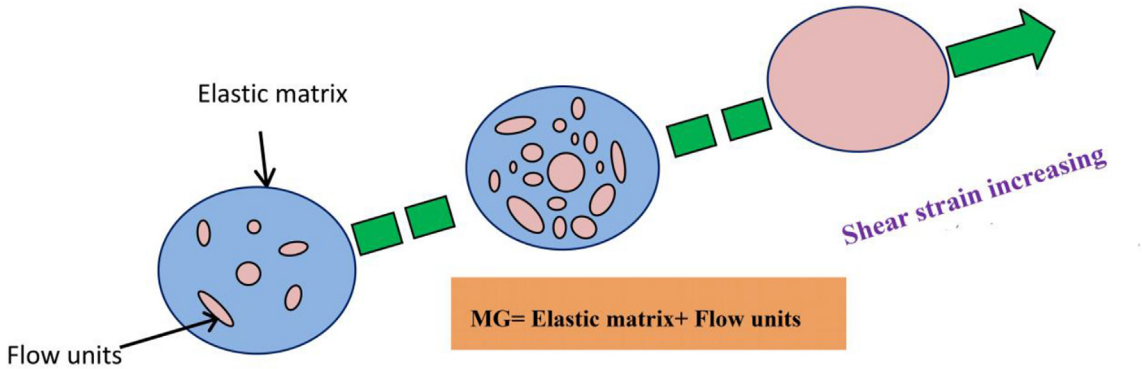

Fig. 6. The embedding structure of MGs and the flow process under shear stress. With shear strain increasing, more flow units are activated and permeated with each other forming local flow.

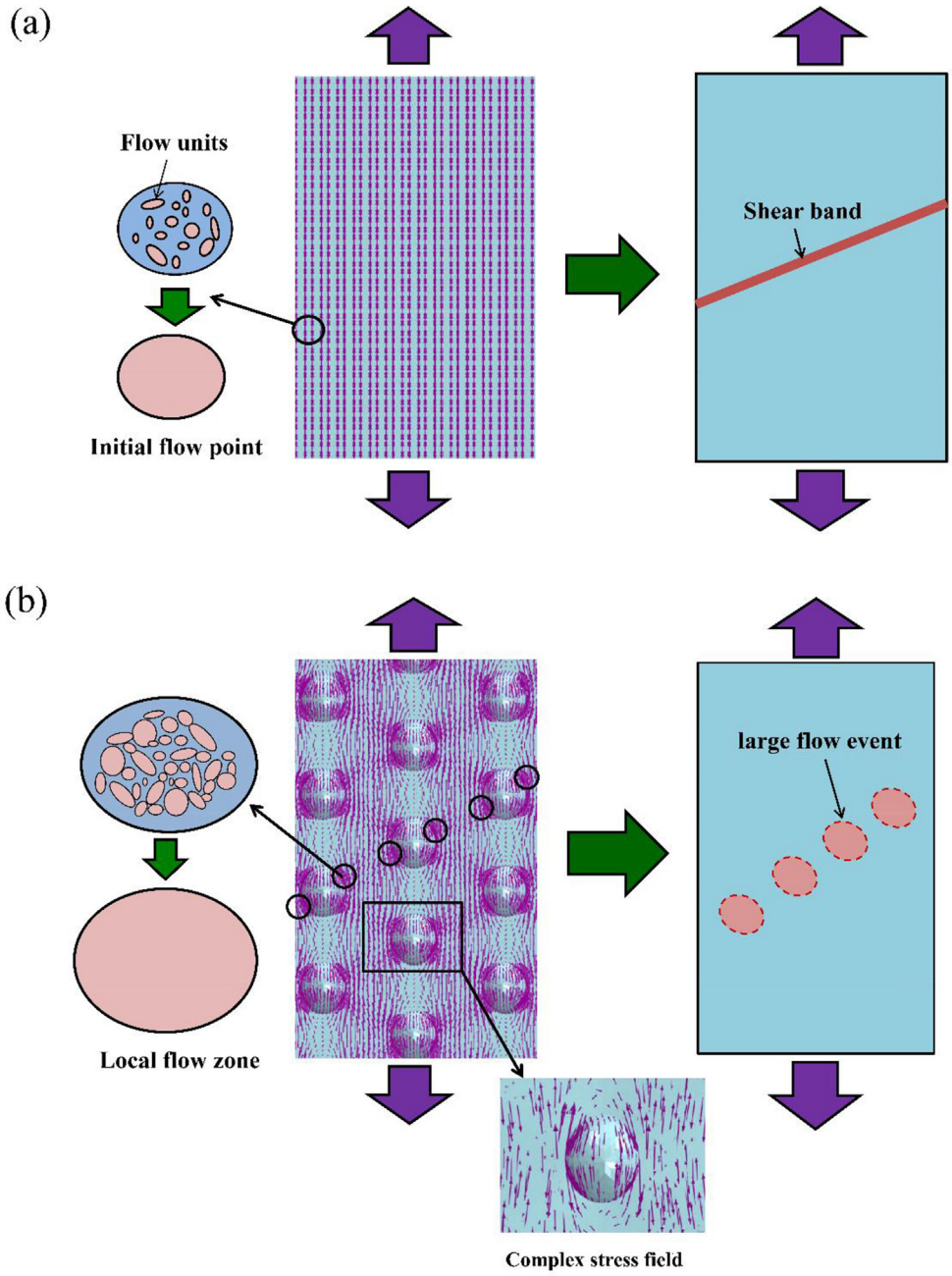

Fig. 7. (a) In the uniform tensile stress field of the as cast specimen, the initial local flow point will rapidly extend into shear band. (b) In the complex stress field of the L-E specimen, more flow units are generated in shear concentration regions and finally permeate with each other, forming local flow. The local flow is constrained by the surrounding complex stress field, becoming large flow event rather than extending into shear band.

surrounded complex stress field, contributing to form a larger local flow. The flow forms influenced by the complex stress field is changed into many large flow events rather than shear bands clusters. Furthermore, it is proved that the shear induced flow is not just constrained in nanosize shear band at room temperature and the flow form is governed by the high shear stress field. Our results may provide guidelines for enhancing the ductility of metallic glasses based on their flow properties.

Acknowledgments

This work is supported by the National Natural Science Foundation of China (Grant Numbers. 11372323, 11302231), MOST 973 of China (No. 2015CB856800), and CAS Key Technology Talent Program.

References

[1] A.L. Greer, Metallic glasses, Science 267 (1995) 1947–1953.
[2] W.L. Johnson, Bulk glass-forming metallic alloys: Science and technology, MRS Bull. 24 (1999) 42–56.
[3] A. Inoue, Bulk amorphous and nanocrystalline alloys with high functional properties, Mater. Sci. Eng. A 304 (2001) 1–10.
[4] W.H. Wang, C. Dong, C.H. Shek, Bulk metallic glasses, Mater. Sci. Eng. R. 44 (2004) 45–89.
[5] A. Inoue, F.L. Kong, S.L. Zhu, F. Al-Marzouki, Peculiarities and usefulness of multicomponent bulk metallic alloys, J. Alloys Compd. 707 (2017) 12–19.
[6] D.C. Hofmann, J.Y. Suh, A. Wiest, et al., Designing metallic glass matrix

composites with high toughness and tensile ductility, Nature 451 (2008) 1085–1089.
[7] C.A. Schuh, T.C. Hufnagel, U. Ramamurty, Mechanical behavior of amorphous alloys, Acta Mater. 55 (2007) 4067–4109.
[8] A.L. Greer, Y.Q. Cheng, E. Ma, Shear bands in metallic glasses, Mater. Sci. Eng. R. 74 (2013) 71–132.
[9] G.N. Yang, B.A. Sun, S.Q. Chen, Y. Shao, K.F. Yao, The multiple shear bands and plasticity in metallic glasses: a possible origin from stress redistribution, J. Alloys Compd. 695 (2017) 3457–3466.
[10] M.M. Trexler, N.N. Thadhani, Mechanical properties of bulk metallic glasses, Prog. Mater. Sci. 55 (2010) 759–839.
[11] Y.H. Liu, G. Wang, R.J. Wang, et al., Super plastic bulk metallic glasses at room temperature, Science 315 (2007) 1385–1388.
[12] J. Schroers, W.L. Johnson, Ductile bulk metallic glass, Phys. Rev. Lett. 93 (2004) 255506.
[13] S.X. Song, H. Bei, J. Wadsworth, T.G. Nieh, Flow serration in a Zr-based bulk metallic glass in compression at low strain rate, Intermetallics 16 (2008) 813–818.
[14] R.D. Conner, Y. Li, W.D. Nix, W.L. Johnson, Shear band spacing under bending of Zr-based metallic glass plates, Acta Mater. 52 (2004) 2429–2434.
[15] B. Sarac, J. Schroers, Designing tensile ductility in metallic glasses, Nat. Commun. 4 (2013) 1–7.
[16] R.T. Qu, M. Calin, J. Eckert, Z.F. Zhang, Metallic glasses: notch-insensitive materials, Scr. Mater. 66 (2012) 733–736.
[17] R.T. Qu, J.X. Zhao, M. Stoica, J. Eckert, Z.F. Zhang, Macroscopic tensile plasticity of bulk metallic glass through designed artificial defects, Mater. Sci. Eng. A 534 (2012) 365–373.
[18] R.T. Qu, Q.S. Zhang, Z.F. Zhang, Achieving macroscopic tensile plasticity of monolithic bulk metallic glass by surface treatment, Scr. Mater. 68 (2013) 845–848.
[19] Q. Wang, Y. Yang, H.C. Jiang, et al., Superior tensile ductility in bulk metallic glass with gradient amorphous structure, Sci. Rep. 4 (2014) 4757.
[20] K.K. Song, S. Pauly, Y. Zhang, et al., Significant tensile ductility induced by cold rolling in $Cu_{47.5}Zr_{47.5}Al_5$ bulk metallic glass, Intermetallics 19 (2011) 1394–1398.
[21] J.H. Luo, F.F. Wu, J.Y. Huang, et al., Super elongation and atomic chain formation in nanosized metallic glass, Phys. Rev. Lett. 104 (2010) 215503.
[22] H. Guo, P.F. Yan, Y.B. Wang, et al., Tensile ductility and necking of metallic glass, Nat. Mater. 6 (2007) 735–739.
[23] D.J. Magagnosc, K.G. Ehrbar, M.R. He, et al., Tunable tensile ductility in metallic glasses, Sci. Rep. 3 (2013) 1096.
[24] D.L. Malandro, D.J. Lacks, Molecular-level mechanical instabilities and enhanced self-diffusion in flowing liquids, Phys. Rev. Lett. 81 (1998) 5576–5579.
[25] D.L. Malandro, D.J. Lacks, Relationships of shear-induced changes in the potential energy landscape to the mechanical properties of ductile glasses, J. Chem. Phys. 110 (1999) 4593–4601.
[26] J. Chattoraj, A. Lemaitre, Elastic signature of flow events in supercooled liquids under shear, Phys. Rev. Lett. 111 (2013) 066001.
[27] Z. Lu, W. Jiao, W.H. Wang, H.Y. Bai, Flow unit perspective on room temperature homogeneous plastic deformation in metallic glasses, Phys. Rev. Lett. 113 (2014) 045501.
[28] Z. Wang, B.A. Sun, H.Y. Bai, Evolution of hidden localized flow during glass-to-liquid transition in metallic glass, Nat. Commun. 5 (2014) 5823.
[29] S. Pauly, S. Gorantla, G. Wang, et al., Transformation-mediated ductility in CuZr-based bulk metallic glasses, Nat. Mater. 9 (2010) 473–477.
[30] C.A. Pampillo, A.C. Reimschuessel, The fracture topography of metallic glasses, J. Mater. Sci. 9 (1974) 718–724.
[31] R.T. Qu, Z.F. Zhang, Compressive fracture morphology and mechanism of metallic glass, J. Appl. Phys. 114 (2013) 193504.
[32] W. Dmowski, T. Iwashita, C.P. Chuang, et al., Elastic heterogeneity in metallic glasses, Phys. Rev. Lett. 105 (2010) 205502.
[33] Z. Wang, P. Wen, L.S. Huo, et al., Signature of viscous flow units in apparent elastic regime of metallic glasses, Appl. Phys. Lett. 101 (2012) 121906.
[34] W.H. Wang, Y. Yang, T.G. Nieh, et al., On the source of plastic flow in metallic glasses: concepts and models, Intermetallics 67 (2015) 81–86.
[35] A.S. Argon, Plastic deformation in metallic glasses, Acta Metall. 27 (1979) 47–58.
[36] C. Fan, P.K. Liaw, C.T. Liu, Atomistic model of amorphous materials, Intermetallics 17 (2009) 86–87.
[37] H. Wagner, D. Bedorf, S. Küchemann, et al., Local elastic properties of a metallic glass, Nat. Mater. 10 (2011) 439–442.
[38] Y.H. Liu, D. Wang, K. Nakajima, et al., Characterization of nanoscale mechanical heterogeneity in a metallic glass by dynamic force microscopy, Phys. Rev. Lett. 106 (2011) 125504.